

- [16] Considering the fitted time-dependent fluorescence $I(t)$ and the calculated mean lifetime at a fixed emission wavelength $[\tau_m(\lambda_e)]$ [17], the total mean lifetime τ_m corresponding to the steady-state fluorescence spectrum was calculated according to Equations 1 and 2 (see Experimental section).
- [17] J. Duhamel, A. S. Jones, T. J. Dickson, *Macromolecules* **2000**, *33*, 6344.
- [18] This trend may also arise from the different intermolecular interactions between the adjacent conjugated rods with the variation in the length of the coil segment [19]. However, the 3D confinement effect of the domains seems to be more important in the fluorescence enhancement of these supramolecular materials, as evidenced by density measurements of the rod segments.
- [19] a) G. Rumbles, I. D. W. Samuel, C. J. Collison, P. F. Miller, S. C. Maratti, A. B. Holmes, *Synth. Met.* **1999**, *101*, 158. b) S. C. J. Meskers, R. A. J. Janssen, J. E. M. Haverkort, J. H. Wolter, *Chem. Phys.* **2000**, *260*, 415.

Confined Surface Plasmons in Gold Photonic Nanocavities**

By *M. Caterina Netti, Steve Coyle, Jeremy J. Baumberg,* Mohammed A. Ghanem, Peter R. Birkin, Phil N. Bartlett, and David M. Whittaker**

The interaction of light with metals is strongly enhanced by texturing their surface on the scale of the optical wavelength. Normally highly reflecting, metals in sub-micrometer architectures such as spheres can show strong absorptions in the visible spectrum^[1–3] due to resonant charge oscillations termed plasmons. However, it is non-trivial to size-select and support such metal spheres in solids. Here we demonstrate a simple scheme to produce large-area colored metal surfaces by completely confining surface plasmons inside gold spherical nanocavities. In contrast to periodic patterning of dielectrics,^[4] metals,^[5,6] or metallodielectrics,^[7] which can produce photonic crystals, here the negative nanocavity curvature localizes the electromagnetic fields into small volumes which can be arranged non-periodically. The microstructured surfaces are formed in a process analogous to “lost wax” casting, by the electrochemical deposition of gold through a template of self assembled latex spheres, generating a wide variety of confining geometries over extended areas of a mechanically robust film. Sharp quantized plasmon resonances are observed in the specular reflection spectra, which correspond to solutions of Maxwell’s equations in a spherical metallic void. Unlike spheres, voids couple strongly to incident light with resonant wavelengths which are widely tunable through the growth morphology, but are omnidirectional. Such nanostruc-

tures enable new optical interactions in reduced dimensions and provide cost-effective tunable spectral filters.

The metallic microstructures were cast by electrochemical deposition through the pores of an array of sub-micrometer polystyrene latex spheres. These were initially crystallized onto a gold-coated glass slide from colloidal solution.^[8,9] The resulting metallic mesh reflects the order of the self-assembled template, allowing convenient control of the pore diameters and local crystalline order. Measurement of the total charge passed allows accurate deposition of the required metal thickness, after which the template can be dissolved in toluene. This last step can be carried out without the shrinkage previously found to cause cracking.^[10] Extending our previous work^[8] to gold nanotextured films, we are now able to devise new geometries for optical plasmon confinement.

By preparing a sample that is graded in thickness, the electrochemical growth can be followed using scanning electron micrographs of the top surface (Fig. 1). Initially the gold forms a hemispherical cavity (i–iv), but the diffusion-reaction limited nature of the aggregation is geometrically hindered by the next layer of latex spheres, which prevents the cavity from completely closing. Instead a three-fold symmetric pattern of interlinked holes form (v–x) connecting the next hemispherical cavities to the layer below. This mesostructure is repeated in subsequent layers above.

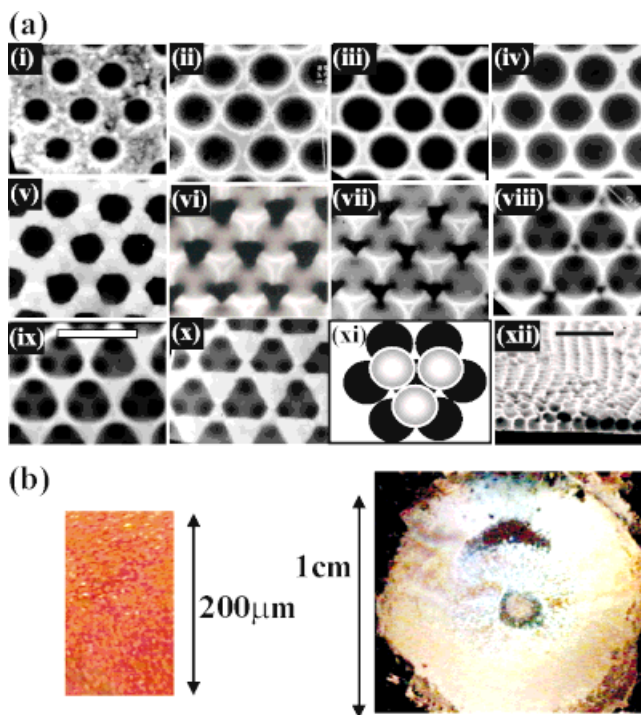


Fig. 1. a) Scanning electron micrographs of the photonic gold nanostructures fabricated with $d = 700$ nm latex spheres. The thickness varies continuously across the sample: i) 50 nm, iv) 350 nm, vii) 700 nm, x) 1100 nm (scale bar is 1 μ m). xi) The lowest void layer (black) and second layer (gray). xii) Cross section (scale bar is 5 μ m). b) Diffuse scatter from the sample surface under white light illumination, exhibiting color changes for different thickness. Left: 100 μ m \times 200 μ m area of uniformly 500 nm thick $d = 500$ nm sample. Right: 1 cm \times 1 cm image of a $d = 700$ nm graded sample—larger crystallites are visible in the center.

[*] Prof. J. J. Baumberg, Dr. M. C. Netti, S. Coyle
Department of Physics and Astronomy, University of Southampton
SO17 1BJ (UK)
E-mail: j.j.baumberg@soton.ac.uk
M. A. Ghanem, Dr. P. R. Birkin, Prof. P. N. Bartlett
Department of Chemistry, University of Southampton
SO17 1BJ (UK)
Dr. D. M. Whittaker
Toshiba Research Europe Ltd
Cambridge, CB4 4WE (UK)

[**] We thank George Attard, Bill Brocklesby, and Jeremy Frey for discussions, the Southampton NanoMaterials Forum, HEFCE JR98SOBA, and EPSRC GR/N37261 for support. MAH thanks the Embassy of the Arab Republic of Egypt, Educational and Cultural Bureau, London, for financial support.

The local optical reflectivity of the macroporous Au films is measured using a white-light laser focused to a 10 μm diameter spot.^[11] Typical reflection spectra at 45° incidence for latex spheres of diameter, $d = 700$ nm, are shown in Figures 2a,b for a range of Au thicknesses, and display strong dips that are not generated by the unpatterned films (dashed). Although

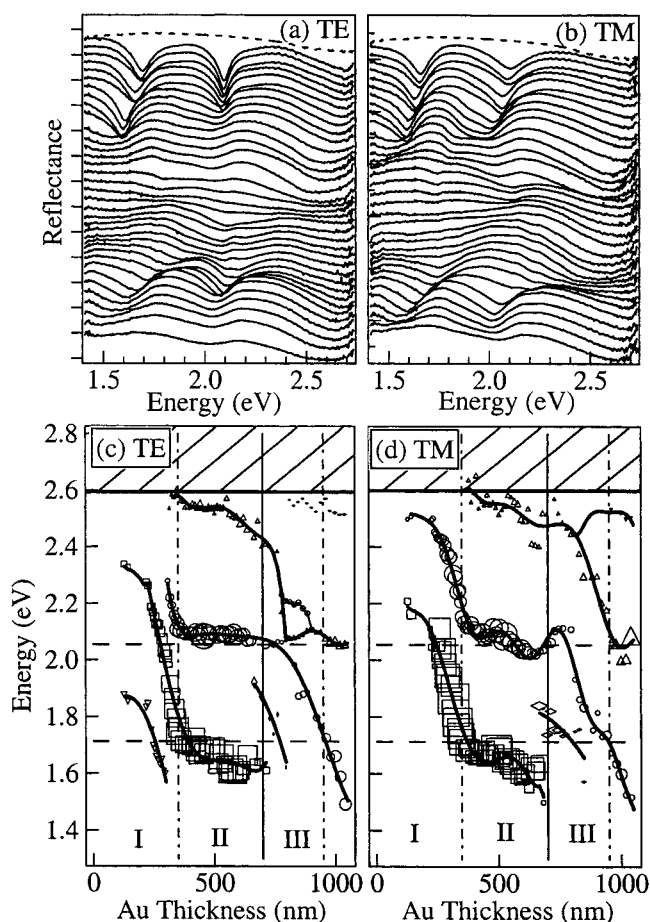


Fig. 2. a,b) Reflectivity spectra on the same sample at different locations (thicknesses 500–1100 nm from top to bottom) for both TE and TM polarized incident light at 45°. The scale is logarithmic, each tick is a factor of 10, and the curves have been offset for clarity. The dotted curve is an unpatterned film electrodeposited under the same conditions. c,d) Extracted mode energies for TM, TE polarizations at 45°. The symbol size indicates the mode sharpness (depth/linewidth). The vertical lines mark the heights of 1/2, 1, 3/2 spheres, and above 2.6 eV planar surface plasmon absorption occurs. The dashed horizontal lines are from a theory of idealized spherical voids.

the short-range order of the latex sphere array can be good (Fig. 1a), the crystal grains here are typically a few micrometers across, resulting in an amorphous microstructure which suppresses diffraction. This is confirmed by the insensitivity of the spectra to the in-plane (azimuthal) orientation of the metallic nanostructure. As the angle of incidence is changed, the resonant dips vary in strength and principal polarization (transverse electric (TE) or transverse magnetic (TM)) axis ratio, but show minimal energy shifts. When we examine more ordered crystallites a complicated structure is seen which becomes dependent on the nanostructure orienta-

tion, to be discussed elsewhere. Extinction ratios in excess of 20 dB are found and up to three resonances seen simultaneously. In particular, a range of film thicknesses (from a half to nearly a full sphere height) are found for which the TE and TM resonances are sharp (<20 nm halfwidths) and coincident. The correlation of the microstructure with these resonant energies confirms that the modes arise from zero-dimensional plasmons trapped inside the Au cups.

Electron microscopy allows direct confirmation of the film thickness, through measurement of the size and shape of the pore openings at the sample surface. The extracted energies of the modes are shown in Figures 2c,d for TE, TM incident polarizations. When the cups in the growing gold film are small, the frequencies change only slowly. However near the half-height thickness, the modes rapidly shift to longer wavelengths (region I). This is exactly the opposite behavior to that expected for interference on a length-scale set by the rim circumference of the nanocavity—the diameter changes rapidly for the thinnest layers and barely changes near the half-height thickness, suggesting that rim plasmons are not observed. Subsequently the mode frequencies change little until close to the full height thickness (region II). Again this insensitivity suggests that the cavity aperture does not directly control the resonance. Only at the interface between two layers of latex spheres does the optical extinction become strong, producing “black” gold. At larger thicknesses the nanostructures repeat, and similar modes are seen once the highly eccentric transition region is passed (region III is similar to I), although the expected periodicity is disturbed by coupling between modes. The modes emerge below the limiting-value of the 2D plasmon frequency for gold, and are not observed on similar Pt or Co mesoporous films. Thus we attribute them to fully localized surface plasmon polaritons inside cups of Au, and suggest that the independence of the mode frequencies in the enclosed nanocavities to the film thickness and angle of incidence, arises from the ability of plasmons to travel around an equatorial circle in the interior.

Full solutions of Maxwell’s equations through photonically patterned metals are complicated by the strength of the coupling between propagating plasmons with different wave-vectors. This is the opposite regime to “weak” coupling found in dielectric photonic crystals^[4] in which a perturbative approach is tractable. Previous work on photonic metals has focused on the use of regular arrays of corrugations or holes of a lateral size much less than the optical wavelength, which produces complex and highly directional performance due to their periodicity.^[5,6,12–14] Here we find that plasmons trapped in spherical voids arranged in amorphous arrays possess simple discrete energy levels. The solution for plasmons on metal spheres is well known, and analytic for diameters small enough to allow a non-retarded approximation (i.e., $d \ll \lambda$).^[15] We extend the solution to spherical metal voids on the scale of the plasmon wavelength ($d \sim \lambda$), which provides an intuitive explanation for our observations. The electromagnetic surface modes can be numerically evaluated by solving the relevant boundary conditions^[16] (predictions marked as horizontal

lines on Figs. 2c,d). The mode frequencies of the localized plasmons depend on the normalized void radius $R = \pi d/\lambda_p$ (λ_p is the 3D plasmon wavelength), and the quantized angular momenta, ($l, m = 0, \pm 1, \dots, \pm l$). As the spherical voids get smaller, the localized plasmon energies increase depending on the angular momentum of each state. Unlike the effect of positive surface curvature on a metal sphere, the negative curvature of the metal void increases the frequency of the plasmons which allows them to couple to external photons. The different bands observed in Figure 2 correspond to localized plasmon states of different angular momentum l , spaced according to the particular spherical curvature set by the void radius. In all our measurements, we indeed only observe the localized modes which have a momentum, $k = l/R$ (tangential to the curved surface) which can couple to photons propagating away from the sample, as expected from wave-vector conservation. Because of the near-spherical void geometry, photons impinging from different directions couple to the same plasmons leading to omni-directional performance. Control of the metallic geometry allows both mode energies and lifetimes to be tuned. The observed frequencies and separations for several experimental void diameters ($R = 1.9, 4.5, 6.5, 9.1$) at thicknesses around the 3/4 sphere height are in good agreement with this idealized spherical model despite the distortions introduced by the apertures at the top of the voids. The reason for this can be seen from the spatial field distribution of the high-angular momentum solutions ($m = l$) for surface plasmons, which are concentrated in lobes on the equatorial plane (Fig. 3a) away from the aperture (as compared to $m < l$, Fig. 3b). Such modes can be excited by both TE and TM polarizations although with different strengths. Further theoretical work to explain the anticrossings and extra perturbed modes seen in the spectra, will be presented elsewhere.

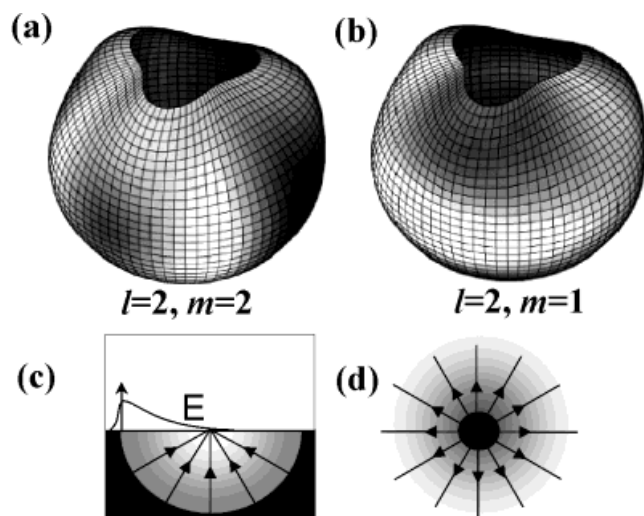


Fig. 3. a,b) Calculated radial electric fields on the surface of the microcavity for $(l,m) = (2,2)$ and $(2,1)$ (on the sphere surface, darker shading shows stronger electric fields). c,d) Schematic radial field profile of the localized plasmons in voids and on spheres.

Localized plasmons are analogous to electrons confined in atoms. The similar structure of Maxwell's and Schrödinger's equations provide similar solutions but on different length-scales, and suggest a range of possible applications for this technology. The negative curvature confinement increases the plasmon energies because a greater electric field overlap is produced in the surrounding air, increasing the electromagnetic energy densities (Fig. 3c). In contrast, the positive curvature metal surface reduces this energy density, resulting in little confinement (Fig. 3d). A second significant difference between metal voids and metal spheres is the momentum required by photons to interact with the localized plasmons. Compared to small spheres that have plasmons which are difficult to tune in frequency, metallic voids with $1.33 < R < 10$ have plasmons in a well-defined cup geometry which are tunable from the ultraviolet (UV) to the near infrared, which strongly interact with impinging light. The strong localization of the surface plasmons removes any restrictive requirements on specifically periodic patterning of the surface. In particular tunable metallic filters and sensors are a strong prospect. In addition, such nano-optical devices have unusual properties such as near-field collimation for chromophores arranged at the optical focus of the microcavities. Indeed we have recently shown that dropping a scanning-near-field optical tip into the spherical voids increases the retro-reflected light by several orders of magnitude. In addition, we are also investigating magnetic photonic mesoporous metals. The ability to easily fabricate, at low cost, a large variety of such photonic metallic structures promises applicability in many diverse areas ranging from biotechnology to optoelectronics.

Received: March 15, 2001
Final version: May 10, 2001

- [1] U. Kreibitz, M. Vollmer, *Optical Properties of Metal Clusters*, Springer, Berlin **1995**.
- [2] R. Averitt, D. Sakar, N. Halas, *Phys. Rev. Lett.* **1997**, *78*, 4217.
- [3] S. J. Oldenburg, J. B. Jackson, S. L. Wescott, N. J. Halas, *Appl. Phys. Lett.* **1999**, *75*, 2897.
- [4] J. D. Joannopoulos, R. D. Meade, J. N. Winn, *Photonic Crystals*, Princeton University Press, Princeton, NJ **1995**.
- [5] T. W. Ebbesen, H. J. Lezec, H. G. Ghaemi, T. Thio, P. A. Wolff, *Nature* **1998**, *391*, 667.
- [6] W. L. Barnes, T. W. Priest, S. C. Kitson, J. R. Sambles, *Phys. Rev. B* **1996**, *54*, 6227.
- [7] W. Y. Zhang, *Phys. Rev. Lett.* **2000**, *84*, 2853.
- [8] P. N. Bartlett, P. R. Birkin, M. A. Ghanem, *Chem. Commun.* **2000**, 1671.
- [9] Z. Zhong, Y. Yin, B. Gates, Y. Xia, *Adv. Mater.* **2000**, *12*, 203.
- [10] J. E. G. J. Wijnhoven, S. J. M. Zevenhuizen, M. A. Hendriks, D. Vanmaekelbergh, J. J. Kelly, W. L. Vos, *Adv. Mater.* **2000**, *12*, 888.
- [11] M. C. Netti, M. B. D. Charlton, G. J. Parker, J. J. Baumberg, *Appl. Phys. Lett.* **2000**, *76*, 991.
- [12] J. A. Porto, F. J. Garcia-Vidal, J. B. Pendry, *Phys. Rev. Lett.* **1999**, *83*, 2845.
- [13] W.-C. Tan, T. W. Preist, J. R. Sambles, N. P. Wanstall, *Phys. Rev. B* **1999**, *59*, 12 661.
- [14] H. F. Ghaemi, T. Thio, D. E. Grupp, T. W. Ebbesen, H. J. Lezec, *Phys. Rev. B* **1998**, *58*, 6779.
- [15] H. Raether, *Surface Plasmons*, Springer, Berlin **1988**.
- [16] A. D. Boardman, *Electromagnetic Surface Modes*, Wiley, Chichester, UK **1982**.